Scaling Theory of Wave Confinement in Classical and Quantum Periodic Systems

Marek Kozoň,[1,2,*] Ad Lagendijk,[1] Matthias Schlottbom,[2] Jaap J. W. van der Vegt,[2] and Willem L. Vos[1,†]
[1]Complex Photonic Systems (COPS), MESA+ Institute for Nanotechnology, University of Twente, P.O. Box 217, 7500 AE Enschede, Netherlands
[2]Mathematics of Computational Science (MACS), MESA+ Institute for Nanotechnology, University of Twente, P.O. Box 217, 7500 AE Enschede, Netherlands

(Received 1 May 2022; accepted 18 August 2022; published 18 October 2022)

Functional defects in periodic media confine waves—acoustic, electromagnetic, electronic, spin, etc.—in various dimensions, depending on the structure of the defect. While defects are usually modeled by a superlattice with a typical band-structure representation of energy levels, determining the confinement associated with a given band is highly nontrivial and no analytical method is known to date. Therefore, we propose a rigorous method to classify the dimensionality of wave confinement. Starting from the confinement energy and the mode volume, we use finite-size scaling to find that ratios of these quantities raised to certain powers yield the confinement dimensionality of each band. Our classification has negligible additional computational costs compared to a band structure calculation and is valid for any type of wave, both quantum and classical, and in any dimension. In the quantum regime, we illustrate our method on electronic confinement in 2D hexagonal boron nitride (BN) with a nitrogen vacancy, in agreement with previous results. In the classical case, we study a three-dimensional photonic band gap cavity superlattice, where we identify novel acceptorlike behavior. We briefly discuss the generalization to quasiperiodic lattices.

DOI: 10.1103/PhysRevLett.129.176401

Completely controlling wave propagation in periodic media is a key challenge that is essential for a large variety of applications [1–15]. An especially interesting type of control is wave confinement achieved by introducing disorder and functional defects into an otherwise periodic medium. The interference of waves in such an altered structure may result in a strong concentration of the energy density inside a small subvolume of the medium. Wave confinement has been investigated for different types of waves and in various settings, e.g., classical mechanics [16], photonics [9,10,17–19], solid state physics [20–24], or magnonics [25,26]. Its applications include sensors, controlled spontaneous emission, and enhanced interactions between hybrid wave types such as sound and light [27–35].

The analysis of spatial concentration of energy in physical systems is in photonics traditionally done via the mode volume [18,36–39] or in condensed matter physics via the participation ratio [16,23,40]. Bands with small mode volume or participation ratio are considered confined while, conversely, bands with large mode volume or participation ratio are taken to be extended [16,18,19,22–24,41]. However, the notion of what specifically is "large" and "small" is in each case determined subjectively as there are no rigorous boundaries imposed by nature.

An alternative method to analyze the wave confinement, multifractality analysis [42–44], is based on the scaling of the participation ratio in the limit of infinitely large supercells. Unfortunately, this approach requires impractically large supercells, which is further compounded by its inability to deal with band folding [45].

Therefore, in this Letter we present a rigorous, derived method to determine the confinement of waves in periodic structures with defects, based on finite-size scaling [58–60]. Rather than extending the supercells toward impractically large sizes, our method determines confinement in moderately large supercells by comparing them to smaller ones. As a consequence, our approach requires only minimal computational overhead and its results are directly applicable to experimentally relevant finite systems. Our technique can be viewed as a more accessible and practical extension of the multifractality concept and is even suited for automated classification.

Superimposing a defect lattice on an unperturbed crystal lattice gives rise to a defect superlattice [6,22,23,61–63]. A unit cell of such a superlattice that contains N^D unit cells, with D the system dimension, is referred to as a supercell of linear size N. For simplicity, we keep here the number of unit cells per supercell the same for all directions. Based on the geometric dimensionality d of the defects, wave bands

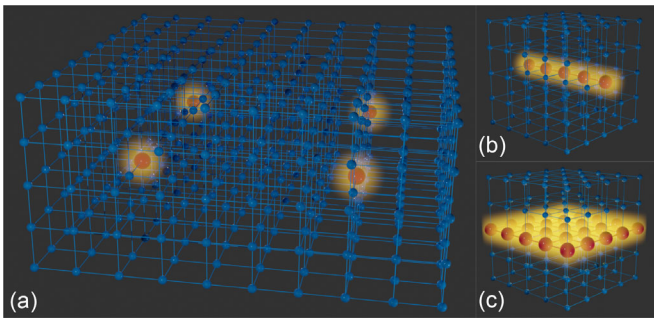

FIG. 1. Illustration of supercells of size $N = 5$ in a $D = 3$ system with various wave confinement dimensionalities c induced by defect geometries of dimensionalities d. Blue spheres correspond to regular unit cells, unit cells containing defects are red, and confined waves are represented by yellow. (a) Four supercells, each containing a point defect akin to a cavity [11], trap waves in all three dimensions, $d = 0$, $c = 3$. (b) Supercell with a linear defect, analogous to an optical waveguide or fiber, $d = 1$, $c = 2$. (c) Supercell with a planar defect, analogous to a 2D electron gas [64], $d = 2$, $c = 1$.

with different confinement dimensionality c arise in the spectrum, as shown in Fig. 1 for an $N = 5$ supercell in $D = 3$ dimensions. The confinement dimensionality c of a wave determines the number of dimensions in which the wave is confined and mathematically corresponds to the codimension of the defect dimensionality: $c = D - d$. We note that introducing defects in every unit cell of the supercell is equivalent to a new periodic structure with no defects ($d = 3$) that supports only extended, unconfined waves ($c = 0$).

Figure 1 represents highly idealized examples of simple defects. Real structures often contain multiple defects of various geometries oriented along different directions. Such complex defect configurations allow for several different confinement dimensionalities c and the problem of assigning the correct c to a given band thus becomes highly nontrivial. In order to understand the confinement in these real structures, a systematic method of identification and classification of confined bands is needed.

To analyze the confinement of waves, one must first determine the physical quantity corresponding to the notion of wave confinement for the given type of physical wave. Without loss of generality, one can make this a real, nonnegative quantity. For example, in electromagnetic systems this quantity could be the energy density, in electronic systems the charge density, and analogously for other waves. We denote this spatially dependent confinement quantity by $W(\mathbf{x})$. To keep the description of our method general, we assume in the following that $W(\mathbf{x})$ has been identified and can be calculated for every band of interest.

For scientifically interesting structures of moderate supercell sizes, the number of bands to be analyzed quickly reaches several hundreds, see, e.g., Refs. [18,19]. It is therefore impractical to analyze the confinement by visually inspecting the spatial distribution of $W(\mathbf{x})$ for each band. These limitations call for a quantitative, automatable method to analyze wave confinement.

We employ $W(\mathbf{x})$ to define the two key quantities for our scaling analysis. First, we consider the mode volume [18,36–39] defined as

$$V_M := \frac{\int_{V_S} W(\mathbf{x}) dV}{\max_{\mathbf{x}\in V_S}\{W(\mathbf{x})\}}, \tag{1}$$

where the integration is over the supercell volume V_S. The mode volume intuitively corresponds to the volume in which the wave is confined. Alternatively, the participation ratio [16,40] can be used [45].

Second, it is important to also consider the problem from the converse point of view: How much energy of the wave is stored in a certain volume? To quantify this notion, we define the confinement energy

$$E_C := \int_{V_C} W(\mathbf{x}) dV, \tag{2}$$

with the integration volume V_C taken as the volume of one unit cell, centered around the defect [45]. An analogous quantity [65] has been introduced [66] to analyze confinement of surface acoustic waves.

We employ normalized quantities

$$\tilde{V} := \frac{V_M}{V_S}, \qquad \tilde{E} := \frac{E_C}{E_S}, \tag{3}$$

where E_S denotes the total amount of energy in the supercell.

For a wave band confined within a cavity we expect simultaneously low $\tilde{V}$ and high $\tilde{E}$, while the opposite (high $\tilde{V}$, low $\tilde{E}$) is expected for a fully extended band. Nevertheless, there are no natural thresholds on how low $\tilde{V}$ and how high $\tilde{E}$ should be for a band to be identified as confined. To overcome this ambiguity, we analyze the behavior of $\tilde{V}$ and $\tilde{E}$ with respect to the variation of the supercell size N, instead of their values themselves. This technique is known as finite-size scaling [58–60].

Our scaling argument is illustrated with the didactic 1D model in Fig. 2. Let us consider a supercell with $N = 4$ with a cavity in its center. For a specific band with certain $\tilde{V}$ and $\tilde{E}$, we are interested in how adding more unit cells to the supercell boundary changes these values, and how these changes differ for a confined band as opposed to an extended band. Therefore, we increase the supercell size to $N = 6$.

A confined band is depicted in Fig. 2(a), with its energy density decaying away from the cavity in the supercell center. Since the size of the cavity to which the wave is confined does not change, it follows that the mode volume

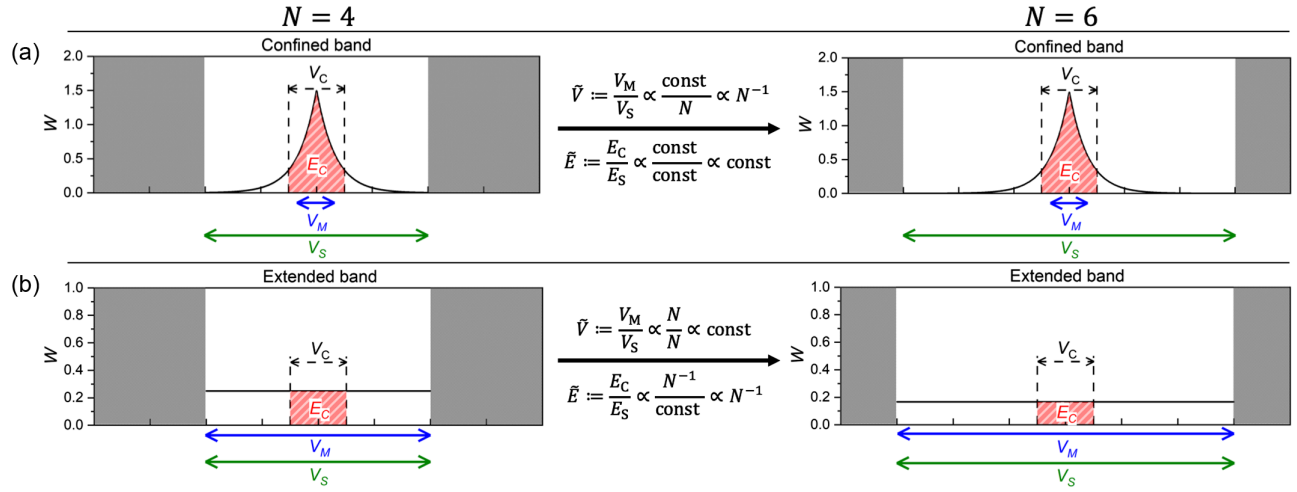

FIG. 2. Illustration of our scaling argument in $D = 1$. An $N = 4$ supercell is transformed into an $N = 6$ supercell by adding unit cells to its boundary. We investigate how the characteristic quantities $\tilde{V}$ and $\tilde{E}$ evolve upon this transition and obtain scaling relations for them. While scaling, we keep the total amount of energy E_S within the supercell constant. (a) Confined band. (b) Extended band.

V_M also remains constant while scaling. However, the supercell volume V_S increases proportionally to N, hence, the normalized quantity $\tilde{V}$ decreases for the confined band as N^{-1}. Since the wave is confined within the cavity, it only "feels" that additional unit cells have been added through its decaying tail. This response clearly approaches zero as $N \to \infty$ and, thus, in this limit $\tilde{E} = \text{const}$.

An extended band is illustrated in Fig. 2(b) by a constant energy density throughout the whole supercell. In this case, the behavior described above is the converse: the volume occupied by the wave in the supercell grows proportionally to the supercell volume, resulting in the scaling $\tilde{V} = \text{const}$. The energy density extends homogeneously throughout the whole supercell and will further spread into the added unit cells as N increases. This leakage decreases the amount of confinement energy E_C within V_C as N^{-1}.

It is straightforward to extend the above scaling analysis to a D-dimensional system. A band with a given confinement dimensionality $0 \le c \le D$ obeys the following scaling relations, in the limit of $N \to \infty$ [45]:

$$\tilde{V} = AN^{-c}, \qquad \tilde{E} = BN^{c-D}. \tag{4}$$

Here, A and B are constants independent of N.

One can calculate $\tilde{V}$ and $\tilde{E}$ from Eqs. (1)–(3) for each band, but because the constants A, B are not known *a priori*, Eqs. (4) cannot be easily inverted to obtain c. To accurately obtain c from our scaling relations, we combine the two equations in (4) into the ratio of the normalized mode volume raised to a judiciously chosen power $\alpha > 0$ and the normalized confinement energy:

$$\frac{\tilde{V}^\alpha}{\tilde{E}} = CN^\kappa, \tag{5}$$

where the exponent κ is given by

$$\kappa = -(\alpha + 1)c + D. \tag{6}$$

By suitably choosing the power α, we can adjust the value of κ so that it is negative for bands with certain c and positive for the other bands. The value of κ, in turn, influences the scaling behavior of these bands as per Eq. (5).

Our technique is illustrated in Fig. 3. Investigating the confinement in a supercell of size N, for every $0 < j \le D$, we have chosen α so that $\kappa < 0$ for all $c \ge j$ and $\kappa > 0$ for all $c < j$. We are now able to distinguish between the bands with $c < j$ and $c \ge j$ by simply tracking the behavior of $\tilde{V}^\alpha/\tilde{E}$ as the supercell grows from a smaller reference size N_0 to the investigated size N. The bands with negative κ will move downward in the graph, while the bands with positive κ will shift upward, in accordance with the Eq. (5). By varying j over all the integer values $0 < j \le D$, this approach allows us to completely classify all wave bands in the spectrum based on their confinement dimensionality.

Equation (5) strictly holds only in the limit of very large N, with subleading order terms in N present for finite

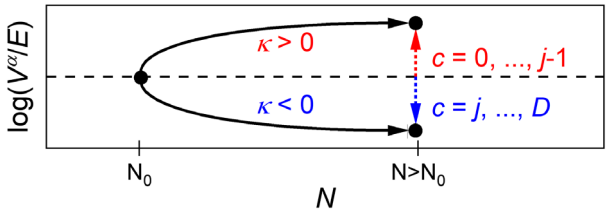

FIG. 3. Flow diagram to identify bands confined in $c \ge j$ dimensions in a D-dimensional medium: the ratio $\tilde{V}^\alpha/\tilde{E}$ versus the system size N. The auxiliary power α is chosen so that $\kappa < 0$ for all $c \ge j$ and $\kappa > 0$ for all $c < j$. The sign of κ determines if $\tilde{V}^\alpha/\tilde{E}$ increases or decreases with growing supercell size.

TABLE I. Auxiliary powers α to classify the confinement in systems of various dimension D. The value of $j \leq D$ indicates the confinement dimensionality being identified, as per Fig. 3.

		D		
		1	2	3
j	3	...	...	$\frac{1}{5}$
	2	...	$\frac{1}{3}$	1
	1	1	3	5

supercell sizes. By following the procedure as outlined in the previous paragraph, there is still some freedom remaining in the choice of the auxiliary power α. This freedom can be utilized to effectively reduce the contribution of these subleading terms, allowing confinement identification already for very small supercells. Nevertheless, since the coefficients corresponding to the subleading terms are generally not known, one cannot eliminate their effect completely, which may show up as misidentification of some bands for small supercells, as we illustrate in an example below. The unique values of α to maximize the accuracy of our technique for $D = 1$, 2, 3 are listed in Table I. For their calculation, see Ref. [45].

In case of the 1D example from Fig. 2, if we choose $\alpha = 1$, corresponding to $D = 1$ and $j = 1$ from Table I, upon plotting $\tilde{V}/\tilde{E}$ versus the supercell size N we will observe that the $c = 1$ confined band moves down, while the $c = 0$ extended band moves up in the flow diagram, analogously to Fig. 3.

We now demonstrate our method on a 2D hexagonal boron nitride (BN) with a nitrogen vacancy representing a pointlike defect [67]. Specifically, we investigate electronic confinement in a supercell of size $N = 5$. The band structure and charge densities of this quantum system were calculated [45] using density functional theory [68] implemented in the VASP code v6.1.1 [69].

The band structure of the system is shown in Fig. 4(a). Since the defect in our $D = 2$ system has point geometry, we only expect two different confinement dimensionalities to appear: the point-confined ($c = 2$) and the extended ($c = 0$) bands. To distinguish between these, we choose $\alpha = \frac{1}{3}$ from Table I and use a reference supercell of size $N_0 = 3$. The plot of $\log(\tilde{V}^{1/3}/\tilde{E})$ for each band in Fig. 4(b) clearly shows that the majority of bands move upward, identifying them as extended ($c = 0$), according to our framework. Additionally, three bands near zero energy move downward and thus correspond to point-confined waves ($c = 2$), in agreement with the findings of Ref. [67].

In our second example, we demonstrate our technique on light confinement in an $N = 4$ supercell of a 3D inverse woodpile photonic crystal with two proximate line defects [18,19,70,71]. The crossing point of these line defects represents a point defect. We study the acceptorlike structure investigated by Ref. [18]. The defects in this

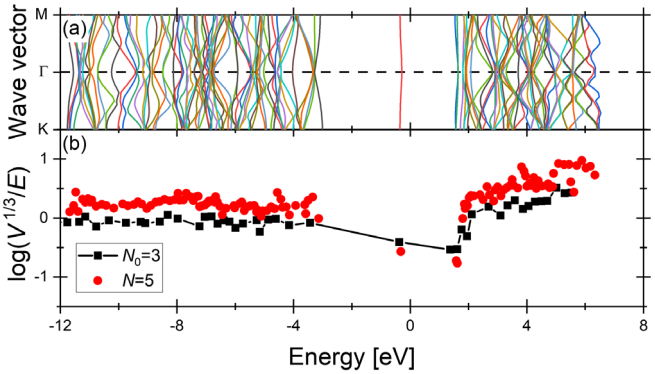

FIG. 4. Our confinement analysis applied to a 2D quantum system: electronic waves in a hexagonal BN with nitrogen deficiency. Zero energy is set at the Fermi level. (a) Band structure of the $N = 5$ supercell, flipped to have an energy abscissa. Bands are distinguished by colors. (b) Scaling analysis of confinement: every band is represented by a point. As the supercell size increases from $N_0 = 3$ to $N = 5$, extended bands move upward, while the three point-confined bands closest to zero energy shift down.

case have more complicated geometry than in the previous example: the system sustains point-confined ($c = 3$) bands, line-confined ($c = 2$) bands, and extended ($c = 0$) bands. The band structure and the energy densities were calculated [45] using the MPB code [72].

Figure 5 depicts the results of our analysis. We unambiguously identify the confinement dimensionality c of most bands. Additionally, several bands, mostly near $\tilde{\omega} \approx 0.5$, appear to be plane confined ($c = 1$). We know, however, that our defect geometry is linear and thus it does not support plane-confined bands. We attribute this discrepancy to the small size of the studied supercell [45].

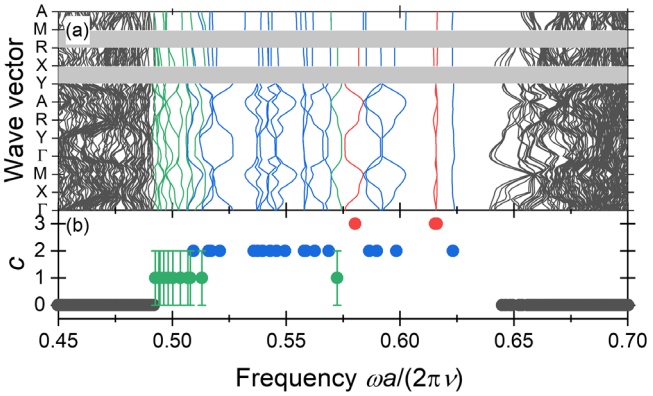

FIG. 5. Scaling analysis of wave confinement in an $N = 4$ supercell of a 3D inverse woodpile photonic crystal with two proximate line defects. The horizontal axis displays the reduced frequency $\tilde{\omega} := \omega a/(2\pi\nu)$, where a is the lattice constant in the y direction and ν denotes the speed of light. (a) Band structure. In the M-A region degenerate bands overlap. (b) Confinement dimensionalities determined by our method for each band. Error bars denote bands assigned to $c = 1$, which should not occur in our structure but appear due to the small size of the supercell.

Nevertheless, our analysis is the first that distinguishes $c = 2$ bands from those with $c = 0$ in a 3D photonic superlattice. We also find three bands (red) with $c = 3$. Visual inspection confirms the point-confined character of the two bands at $\tilde{\omega} \approx 0.62$. We therefore discover point-confined bands in an acceptorlike 3D inverse woodpile structure, thus disproving earlier claims [18] that such bands do not exist. For detailed discussion of the third red band, see Ref. [45].

Reference [19] has shown that in higher dimensional structures such as 3D inverse woodpiles there is no direct correlation between dispersion and coupling in a given direction and thus one cannot assess confinement by analyzing band dispersion. Our method is able to analyze confinement in such structures where the dispersion arguments fail. Furthermore, our technique is not limited to "defect" superlattices in terms of "impurity." Any superlattice superimposed on another lattice can be analyzed by our technique. This is the case for, e.g., Lieb lattices or other so-called flat-band lattices [73,74]. Our technique is also directly applicable to quasicrystals by analyzing their periodic approximants, which, based on Refs. [75,76], exhibit defect properties virtually identical to their parent quasicrystals.

In this Letter, we describe a systematic scaling theory to analyze wave confinement in periodic superlattices, applicable to any type of physical waves. Already in one of the studied examples our technique uncovers physically new results, thus showcasing its power. Our method is directly applicable to actively researched periodic and quasiperiodic structures and for optimization algorithms aiming to minimize or maximize specific types of wave confinement.

The data used for this publication are available [77] via the open-access repository Zenodo that is developed under the European OpenAIRE program and operated by CERN.

We thank Geert Brocks and Menno Bokdam for access to the CMS cluster with VASP code to perform DFT calculations. We also thank Geert Brocks for recommending hexagonal BN to illustrate our method. We thank Sjoerd Hack for the introduction into the MPB software, and Lars Corbijn van Willenswaard, Manashee Adhikary, and Allard Mosk for stimulating discussions on wave physics. This research is supported by the NWO-CSER program, project "Understanding the absorption of interfering light for improved solar cell efficiency" under the Poject No. 680.93.14CSER035; the NWO-JCER program, project "Accurate and Efficient Computation of the Optical Properties of Nanostructures for Improved Photovoltaics" under the Project No. 680-91-084; the NWO-GROOT program, project "Self-Assembled Icosahedral Photonic Quasicrystals with a Band Gap for Visible Light" under the Project No. OCENW.GROOT.2019.071; the NWO-TTW program P15-36 "Free-Form Scattering Optics" (FFSO); and the MESA+ Institute for Nanotechnology, section Applied Nanophotonics (ANP).

*Corresponding author.
m.kozon@utwente.nl
†Corresponding author.
w.l.vos@utwente.nl

[1] P. Markoš and C. M. Soukoulis, *Wave Propagation: From Electrons to Photonic Crystals and Left-Handed Materials* (Princeton University Press, Princeton, NJ, 2008).
[2] M. Fink, D. Cassereau, A. Derode, C. Prada, P. Roux, M. Tanter, J.-L. Thomas, and F. Wu, Rep. Prog. Phys. **63**, 1933 (2000).
[3] Z. Liu, X. Zhang, Y. Mao, Y. Y. Zhu, Z. Yang, C. T. Chan, and P. Sheng, Science **289**, 1734 (2000).
[4] M. Maldovan, Nature (London) **503**, 209 (2013).
[5] S. A. Cummer, J. Christensen, and A. Alù, Nat. Rev. Mater. **1**, 16001 (2016).
[6] V. V. Kruglyak, S. O. Demokritov, and D. Grundler, J. Phys. D **43**, 264001 (2010).
[7] K. Wagner, A. Kákay, K. Schultheiss, A. Henschke, T. Sebastian, and H. Schultheiss, Nat. Nanotechnol. **11**, 432 (2016).
[8] K. Klyukin, L. L. Tao, E. Y. Tsymbal, and V. Alexandrov, Phys. Rev. Lett. **121**, 056601 (2018).
[9] D. M. Callahan, K. A. W. Horowitz, and H. A. Atwater, Opt. Express **21**, 30315 (2013).
[10] A. Tandaechanurat, S. Ishida, D. Guimard, M. Nomura, S. Iwamoto, and Y. Arakawa, Nat. Photonics **5**, 91 (2011).
[11] M. Aspelmeyer, T. J. Kippenberg, and F. Marquardt, Rev. Mod. Phys. **86**, 1391 (2014).
[12] A. F. Koenderink, A. Alù, and A. Polman, Science **348**, 516 (2015).
[13] W. Li and S. Fan, Opt. Express **26**, 15995 (2018).
[14] J. Wang, F. Sciarrino, A. Laing, and M. G. Thompson, Nat. Photonics **14**, 273 (2020).
[15] R. Uppu, M. Adhikary, C. A. M. Harteveld, and W. L. Vos, Phys. Rev. Lett. **126**, 177402 (2021).
[16] F. Arceri and E. I. Corwin, Phys. Rev. Lett. **124**, 238002 (2020).
[17] K. Busch, G. von Freymann, S. Linden, S. Mingaleev, L. Tkeshelashvili, and M. Wegener, Phys. Rep. **444**, 101 (2007).
[18] L. A. Woldering, A. P. Mosk, and W. L. Vos, Phys. Rev. B **90**, 115140 (2014).
[19] S. A. Hack, J. J. W. van der Vegt, and W. L. Vos, Phys. Rev. B **99**, 115308 (2019).
[20] E. N. Economou, *The Physics of Solids*, Graduate Texts in Physics (Springer, Berlin, Heidelberg, 2010).
[21] G. Shao, J. Phys. Chem. C **112**, 18677 (2008).
[22] C. Pashartis and O. Rubel, Phys. Rev. Applied **7**, 064011 (2017).
[23] C. Pashartis and O. Rubel, Phys. Rev. B **96**, 155209 (2017).
[24] J. Zhang, C.-Z. Wang, Z. Z. Zhu, and V. V. Dobrovitski, Phys. Rev. B **84**, 035211 (2011).
[25] *Spin Wave Confinement: Propagating Waves*, 2nd ed., edited by S. O. Demokritov (Pan Stanford Publishing, Singapore, 2017).
[26] E. V. Tartakovskaya, M. Pardavi-Horvath, and R. D. McMichael, Phys. Rev. B **93**, 214436 (2016).
[27] E. Krioukov, D. J. W. Klunder, A. Driessen, J. Greve, and C. Otto, Opt. Lett. **27**, 512 (2002).

[28] T. Baba, Nat. Photonics **2**, 465 (2008).
[29] S. Noda, A. Chutinan, and M. Imada, Nature (London) **407**, 608 (2000).
[30] J. M. Gérard, B. Sermage, B. Gayral, B. Legrand, E. Costard, and V. Thierry-Mieg, Phys. Rev. Lett. **81**, 1110 (1998).
[31] *Single Quantum Dots: Fundamentals, Applications, and New Concepts*, edited by P. Michler, Topics in Applied Physics Vol. 90 (Springer-Verlag, Berlin, Heidelberg, New York, 2003).
[32] J. P. Reithmaier, G. Sęk, A. Löffler, C. Hofmann, S. Kuhn, S. Reitzenstein, L. V. Keldysh, V. D. Kulakovskii, T. L. Reinecke, and A. Forchel, Nature (London) **432**, 197 (2004).
[33] T. Yoshie, A. Scherer, J. Hendrickson, G. Khitrova, H. M. Gibbs, G. Rupper, C. Ell, O. B. Shchekin, and D. G. Deppe, Nature (London) **432**, 200 (2004).
[34] E. Peter, P. Senellart, D. Martrou, A. Lemaître, J. Hours, J. M. Gérard, and J. Bloch, Phys. Rev. Lett. **95**, 067401 (2005).
[35] P. Russell, E. Marin, A. Diez, S. Guenneau, and A. Movchan, Opt. Express **11**, 2555 (2003).
[36] O. Painter, R. K. Lee, A. Scherer, A. Yariv, J. D. O'Brien, P. D. Dapkus, and I. Kim, Science **284**, 1819 (1999).
[37] C. Sauvan, J. P. Hugonin, I. S. Maksymov, and P. Lalanne, Phys. Rev. Lett. **110**, 237401 (2013).
[38] P. T. Kristensen, R.-C. Ge, and S. Hughes, Phys. Rev. A **92**, 053810 (2015).
[39] E. A. Muljarov and W. Langbein, Phys. Rev. B **94**, 235438 (2016).
[40] R. G. S. El-Dardiry, S. Faez, and A. Lagendijk, Phys. Rev. B **86**, 125132 (2012).
[41] K. J. Vahala, Nature (London) **424**, 839 (2003).
[42] H. Aoki, J. Phys. C **16**, L205 (1983).
[43] M. Janssen, Phys. Rep. **295**, 1 (1998).
[44] S. Faez, A. Strybulevych, J. H. Page, A. Lagendijk, and B. A. van Tiggelen, Phys. Rev. Lett. **103**, 155703 (2009).
[45] See Supplemental Material at http://link.aps.org/supplemental/10.1103/PhysRevLett.129.176401 for additional considerations, derivation of our method, details on its applicability and advantages over multifractality, as well as specifications of the performed numerical calculations. It includes Refs. [46–57].
[46] W. Dörfler, in *Photonic Crystals: Mathematical Analysis and Numerical Approximation*, Oberwolfach Seminars Vol. 42 (Springer Basel, Basel, 2011).
[47] W. Ku, T. Berlijn, and C.-C. Lee, Phys. Rev. Lett. **104**, 216401 (2010).
[48] S. G. Mayo, F. Yndurain, and J. M. Soler, J. Phys. Condens. Matter **32**, 205902 (2020).
[49] K. Busch, S. F. Mingaleev, A. Garcia-Martin, M. Schillinger, and D. Hermann, J. Phys. Condens. Matter **15**, R1233 (2003).
[50] N. Marzari, A. A. Mostofi, J. R. Yates, I. Souza, and D. Vanderbilt, Rev. Mod. Phys. **84**, 1419 (2012).
[51] N. Hurley and S. Rickard, IEEE Trans. Inf. Theory **55**, 4723 (2009).
[52] J. P. Perdew, K. Burke, and M. Ernzerhof, Phys. Rev. Lett. **77**, 3865 (1996).
[53] G. Kresse and D. Joubert, Phys. Rev. B **59**, 1758 (1999).
[54] R. Hillebrand, S. Senz, W. Hergert, and U. Gösele, J. Appl. Phys. **94**, 2758 (2003).
[55] M. D. Leistikow, A. P. Mosk, E. Yeganegi, S. R. Huisman, A. Lagendijk, and W. L. Vos, Phys. Rev. Lett. **107**, 193903 (2011).
[56] W. Setyawan and S. Curtarolo, Comput. Mater. Sci. **49**, 299 (2010).
[57] L. F. Richardson, Phil. Trans. R. Soc. A **226**, 299 (1927).
[58] E. Abrahams, P. W. Anderson, D. C. Licciardello, and T. V. Ramakrishnan, Phys. Rev. Lett. **42**, 673 (1979).
[59] P. Sheng, *Introduction to Wave Scattering, Localization, and Mesoscopic Phenomena*, 2nd ed., Springer Series in Materials Science Vol. 88 (Springer, Berlin, New York, 2006).
[60] K. Slevin, P. Markoš, and T. Ohtsuki, Phys. Rev. Lett. **86**, 3594 (2001).
[61] W. L. Bragg and E. J. Williams, Proc. R. Soc. A **145**, 699 (1934).
[62] H. A. Bethe, Proc. R. Soc. A **150**, 552 (1935).
[63] *Semiconductor Superlattices: Growth and Electronic Properties*, edited by H. T. Grahn (World Scientific, Singapore, River Edge, NJ, 1995).
[64] T. Ando, A. B. Fowler, and F. Stern, Rev. Mod. Phys. **54**, 437 (1982).
[65] Termed SAW-likeness coefficient.
[66] D. Nardi, F. Banfi, C. Giannetti, B. Revaz, G. Ferrini, and F. Parmigiani, Phys. Rev. B **80**, 104119 (2009).
[67] B. Huang and H. Lee, Phys. Rev. B **86**, 245406 (2012).
[68] P. Kratzer and J. Neugebauer, Front. Chem. **7**, 106 (2019).
[69] G. Kresse and J. Furthmüller, Comput. Mater. Sci. **6**, 15 (1996).
[70] K. M. Ho, C. T. Chan, C. M. Soukoulis, R. Biswas, and M. Sigalas, Solid State Commun. **89**, 413 (1994).
[71] D. Devashish, O. S. Ojambati, S. B. Hasan, J. J. W. van der Vegt, and W. L. Vos, Phys. Rev. B **99**, 075112 (2019).
[72] S. G. Johnson and J. D. Joannopoulos, Opt. Express **8**, 173 (2001).
[73] S. Mukherjee, A. Spracklen, D. Choudhury, N. Goldman, P. Öhberg, E. Andersson, and R. R. Thomson, Phys. Rev. Lett. **114**, 245504 (2015).
[74] D. Leykam, A. Andreanov, and S. Flach, Adv. Phys: X **3**, 1473052 (2018).
[75] K. Wang, S. David, A. Chelnokov, and J. M. Lourtioz, J. Mod. Opt. **50**, 2095 (2003).
[76] D. N. Chigrin and A. V. Lavrinenko, in *Applications of Metamaterials*, edited by F. Capolino (CRC Press, Boca Raton, FL, 2009).
[77] M. Kozoň, A. Lagendijk, M. Schlottbom, J. W. W. van der Vegt, and W. L. Vos, Zenodo repository, 10.5281/zenodo.6783107.